

NEW SEISMIC ISOLATION DESIGN FOR URBAN TUNNELS IN CONSIDERATION OF SLIP AND ITS APPLICATION TO AN ACTUAL SHIELD-DRIVEN TUNNEL

Takeyasu SUZUKI

Chuo Fukken Consultants Co., Ltd., 2-11, Nihonbashi Oodenma-cho, Cuo-ku, TOKYO 103-0011, Japan

Isao TAKATORI

Public Works Research Center, 1-6-4, Titoh, Taitoh-ku, TOKYO 110-0016, Japan

Ichiro OKADA

Nippon Civic Engineering Consultant Co., Ltd., Nishi-nippori, Arakawa-ku, TOKYO 116-0013, Japan

Ryoji HAGIWARA

Chiba National Highway Work Office, Kanto Regional Development Bureau, Ministry of Land, Infrastructure and Transport, Japan, 5-27-1, Tendai, Inage-ku, Chiba-shi, CHIBA 263-0016, Japan

ABSTRACT: A new seismic isolation technology in which a slip easily occurs between a structure and its peripheral soil or back-filling material has been developed. Such slip takes place by coating the outer surface of structure with a particular silicone paint of water emulsion type with kinetic friction coefficients as low as 0.15. In this paper, seismic design method of urban tunnels in consideration of slip is described first. Then, seismic isolation design is applied to an actual shield-driven tunnel. Seismic isolation design is conducted, focusing on the tunnel portion at connections with vertical shafts. In this design, authors propose the combined use of an isolation layer and segments coated with slipping material, for the purpose of minimizing cost and improving isolation effect. As a result, this technology is proven to be more effective and less expensive than the conventional measures.

1 INTRODUCTION

The Hyogo-ken Nanbu Earthquake of January 1995 damaged not only building and bridge structures but underground structures, some of which such as the Daikai Station on the Kobe Rapid Transit Railway were heavily damaged (Suzuki 1996). It is essential to guarantee the operation of communications, electricity, gas and water supply, and other lifelines in regions struck by large earthquakes. To achieve this goal, the safety from strong earthquakes of utility tunnels that are typical underground structures provided to concentrate these lifeline services should be preserved. In addition, while the earthquake resistance of underground structures must be improved, the public is demanding that the cost of their construction be reduced.

The seismic isolation structure that was developed for underground structures is a structure that can sharply reduce the effect of earthquakes by forming a flexible seismic isolation layer around the outer periphery of an underground structure to insulate the underground structure from deformation of its peripheral ground (Suzuki & Tamura 1995). The research on seismic isolation for underground structures was initiated by a few engineers individually at the end of 1980s (Suzuki 1990, Takeuchi 1994, Kawashima 1989). Right after the earthquake, the Public Works Research Institute of the Ministry of Construction, the Public Works Research Center and 17 private companies have

commenced a three-year joint research project to develop the seismic isolation technology for underground structures. The design method was established, as well as the development of seismic isolation materials and construction methods using these materials, for the seismic isolation structure of underground structures. They were compiled and published in September 1998 as "The Underground Structure Seismic Isolation Design Method Manual (Draft)" (PWRI et al. 1998).

This technology was applied to the connections with both a departure and an arrival vertical shafts of shield-driven tunnel, in the construction of the No.1 Nakagawa utility tunnel, Nagoya (Unjoh et al. 1999). The seismic isolation design for the tunnel was conducted in 1988 and its construction work was carried out at the departure shaft in 1999 and at the arrival shaft in 2000. The effectiveness of the completed isolation structure was verified by conducting a large scale in-situ loading experiment (Unjoh et al. 2000).

The largest problem in this technology, however, is costliness of the isolation material, which is a mixture of silicone rubber material and fly ash. In order to reduce construction cost, therefore, a new seismic isolation system, in which a slip easily occurs between a structure and its peripheral soil or back-filling material by coating the outer surface of the structure with particular paints, has been developed (Suzuki & Katsukawa 2001a).

2 ELASTIC SEISMIC ISOLATION LAYER AND SLIP MATERIAL

The typical material to form elastic seismic isolation layer is the silicone-based isolation material. By mixing two types of liquid A and B immediately before injection, the injected material that filled a void becomes solid rubber in the underground circumstance. Liquid A is the mixture of silicone oil and fly ash, in which fly ash is a filler used to increase the volume. Liquid B, on the other hand, is the catalyst. This isolation material is elastic, shear modulus of which can be controlled. Fig.1 shows shear moduli obtained from hollow cylindrical dynamic simple shear tests on the silicone-based isolation material, SISMO. There is no strain dependency in shear moduli as shown in the figure. SISMO-1 through 7 in the figure denotes a product number for the seismic isolation material, where numbers 1 through 7 at the end mean values of shear modulus in kgf/cm^2 .

The slip material developed for underground structures is a particular silicone paint of water emulsion type. Photo.1 shows the spray coating on shield segments with the paint. Segments coated with such slip material are called "slip segments" in this paper. When backfilling materials are injected during shield driving to a tail void, which exists in between segments and their peripheral ground, the paint absorbs water from backfilling materials or its peripheral ground. A lubricant layer composed of fillers with small particles and water is formed between a film of the paint and the outer surface of segments. Kinetic friction coefficients of the material obtained by hollow cylindrical dynamic shear tests are summarized in Fig.2. As shown in the figure, It is clear that the coefficient is dependent on effective confined pressure. The kinetic friction coefficient used in seismic isolation design, therefore, is given by the approximation formula in the followings (Suzuki & Katsukawa 2001b).

$$\mu = 0.142 + 0.615 \exp(13.941\sigma) \quad (1)$$

where, μ and σ denotes kinetic friction coefficient and effective confining pressure, respectively.

3 SEISMIC ISOLATION DESIGN METHOD IN CONSIDERATION OF SLIP

The method of seismic isolation design in consideration of slip on the outer surface of segments is fundamentally identical with that applied to the seismic isolation layer. The computer code "EASIT", which is a computer program of static analysis based on axisymmetric finite element model, is used in the design (Suzuki 1996). Fig.3 illustrates a schematic representation of the

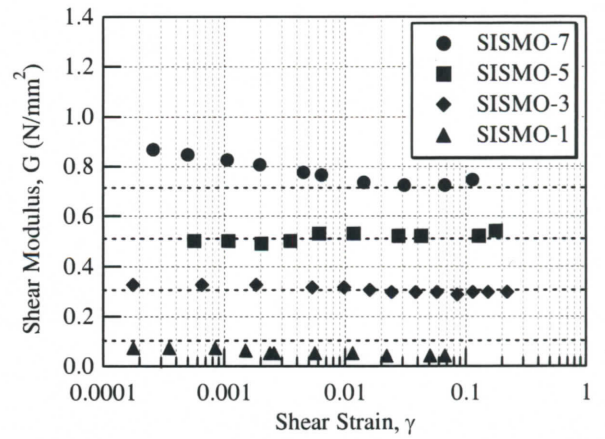


Fig.1 Strain-dependent shear moduli of silicone-based seismic isolation material (SISMO).



Photo.1 Spray coating on shield segments with slip material.

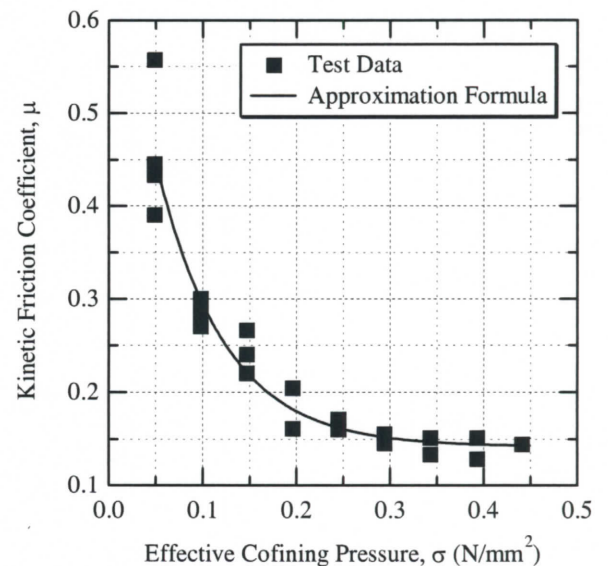


Fig.2 Kinetic friction coefficients of slip material axisymmetric model.

axisymmetric finite element model. In the upper part of the figure, a tunnel is constructed crossing the boundary between a soft soil deposit and a stiff soil deposit. The lower part of the figure represents

the axisymmetric modeling of the ground and tunnel condition in the upper part, in which a tunnel center line is set to be a symmetric axis. It is essential, therefore, that a special consideration should be taken in modeling the effects of ground surface, boundary conditions and seismic load. Then, if a method to convert seismic load in the axisymmetric model to make ground displacement around a tunnel equal in both the upper and lower figures is defined, a simplified procedure, evaluating three-dimensional interaction effects around a tunnel, can be developed. Such a conversion technique was developed and it was coded as the computer program "EASIT" (Suzuki 1996). Thus, the interaction between a tunnel body and surrounding soil can be rigorously evaluated by finite elements with a specified stress-strain relationship.

A slip on the outer surface of segments is taken into consideration by applying a bilinear approximation to the shear stress - strain relationship of thin finite elements covering slip segments. The approximation is illustrated in Fig.4, in which τ_f denotes the critical shear stress, which is coincident with frictional stress given in the following equation:

$$\tau_f = \mu \cdot \sigma \quad (2)$$

where, μ and σ denotes kinetic friction coefficient and effective confining pressure, respectively. In the seismic isolation design, the effective confining pressure at a tunnel center is calculated first. Then, a kinetic friction coefficient of slip segments adopted is calculated using equation (1). Iteration analyses are carried out with a judgment whether a slip occurs or not on the outer surface of slip segments.

Fig.5 shows a schematic illustration to demonstrate a procedure of analysis conducted in the seismic isolation design. Prior to an axisymmetric finite element analysis using EASIT, earthquake response analyses of surface deposits are carried out first, as shown in Fig.5(a). These are one-dimensional multiple reflection analyses with eqi-linear technique. Then, the earthquake input motion at bedrock (denoted by E+F in the figure) and values of soil stiffness and damping factor of surface deposits can be obtained. The multiple degree of freedom system (MDOF) is formed in the next step and modal analysis is carried out as shown in Fig.5(b). Then, a single degree of freedom system (SDOF) for fundamental mode of vibration of the surface deposit is derived. Static external forces or seismic accelerations loaded to the axisymmetric model is calculated, by multiplying response maximum acceleration obtained by the SDOF system by the

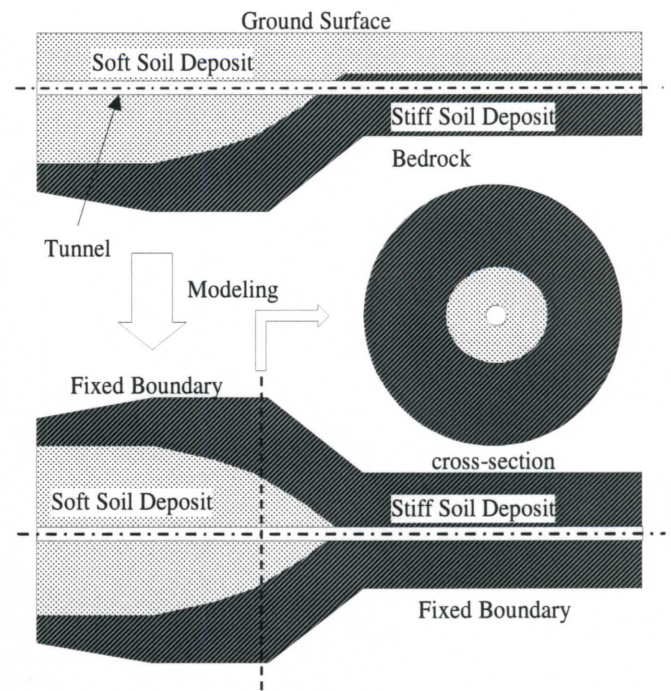


Fig.3 Schematic illustration for axisymmetric modeling used in EASIT

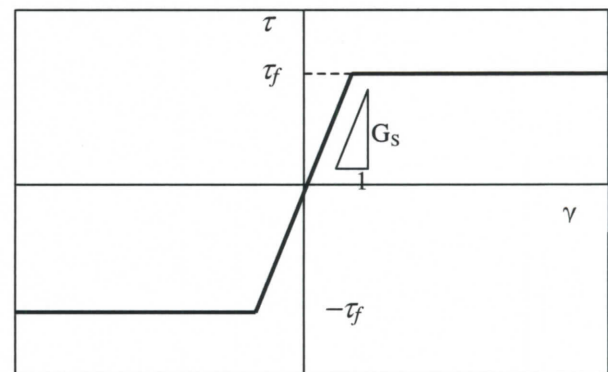


Fig.4 Bilinear shear stress - strain relationship for elements covering slip segments

modal vectors as shown in Fig.5(c).

4 GROUND AND TUNNEL CONDITIONS

The seismic isolation design method shown in the previous chapter was applied to the shield-driven tunnel planned as a utility tunnel in Chiba National Highway Work Office, Kanto Regional Development Bureau, Ministry of Land, Infrastructure and Transport, Japan. The outer diameter of the tunnel is 5450 mm. The thickness of shield segments is 275 mm. Fig.6 shows the longitudinal section which illustrates soil profiles and a longitudinal alignment of the shield-driven tunnel, including vertical shafts. The total length of the tunnel is 5.4 km. The construction of seven shafts, which are composed of 2 departure (E1T1, E7T7), 1 arrival (E4T4) and 4 intermediate shafts (E2T2, E3T3, E5T5 and E6T6), are planned in this

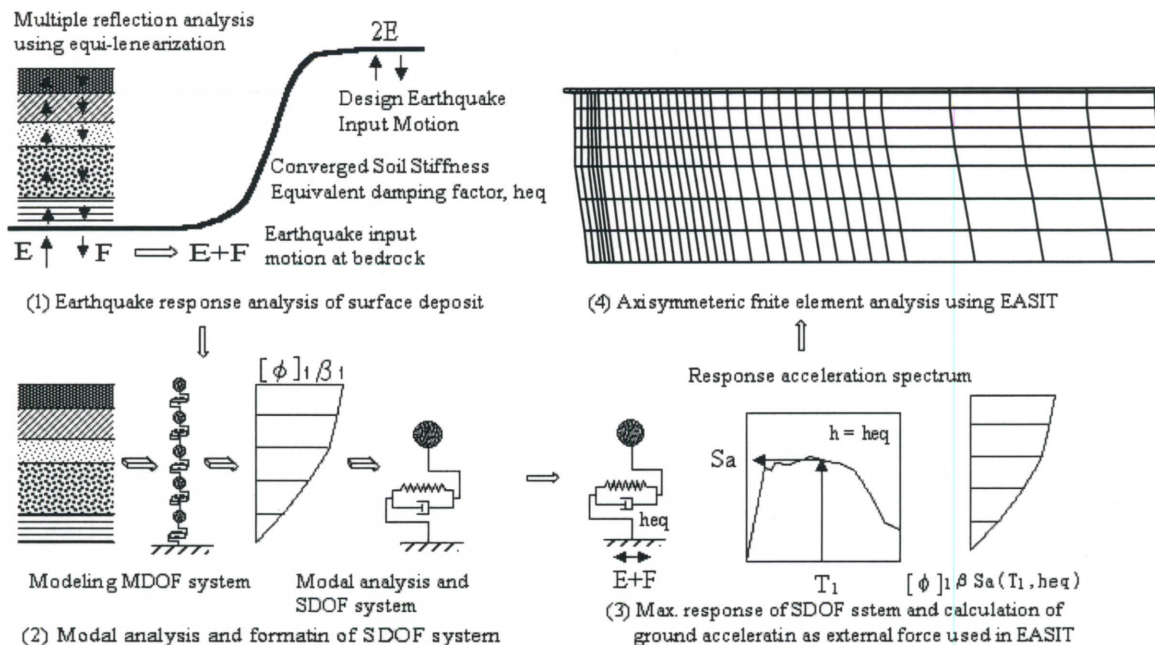


Fig.5 Flow of analytical procedure conducted in the seismic isolation design

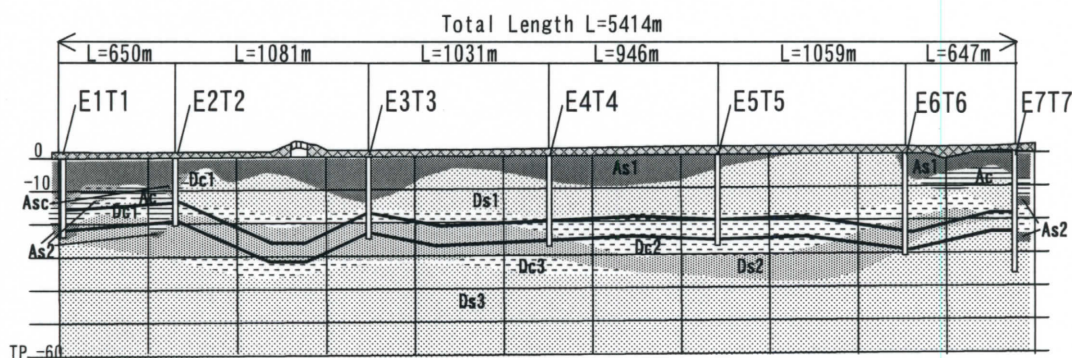


Fig.6 Longitudinal section to represent soil profiles and tunnel alignment

section as shown in the figure. The tunnel is aligned deeply, in order to avoid the influence of liquefaction in shallow sand layers, A_{s1} and D_{s1} and the tunnel is driven through diluvial layers. The earthquake resistant performance of the tunnel, therefore, is relatively high in the ordinary tunnel portion, even though a large earthquake motion is set as a seismic input in a seismic design. The seismic performance against a large earthquake for the tunnel portion at a connection with a vertical shaft, on the contrary, is not necessarily high in general. The authors made the seismic isolation design, therefore, only focusing on such connections.

5 EARTHQUAKE RESPONSE ANALYSES

Earthquake response analyses of surface soil deposits were carried out using a representative soil profile close to each vertical shaft. Input earthquake motions used in the analyses are illustrated in Fig.7. These are usually adopted in seismic design of road bridges as Level 2 earthquake input motions. The TYPE-1 motion denotes a large earthquake motion

occurred at plate boundary deep in the ocean. The TYPE-2 earthquake motion, on the contrary, is the motion originated from a near-field earthquake. Both types of earthquake input motions are considered in the seismic design.

Results of earthquake response analyses of surface soil deposit at the vertical shaft, E7T7 are illustrated in Fig.8, in order to describe representative results of analyses at 7 shafts. Converged shear moduli shown in (b) in the figure were used in the formation of a MDOF system for modal analysis and for an axisymmetric finite element model. Converged damping factors, on the contrary, were used to calculate the equivalent damping factors, h_{eq} for a SDOF system of fundamental mode of shear vibration. The predominant period of the SDOF system or surface soil deposit at E7T7 is 1.63 s for TYPE-I and 1.65 for TYPE-II earthquake motions. The equivalent damping factor, h_{eq} is 0.13 for TYPE-I and 0.14 for TYPE-II earthquake motions. Then, ground acceleration profiles shown in Fig.8(d) was obtained by SDOF analyses. In this case, there is no large difference of acceleration profile between

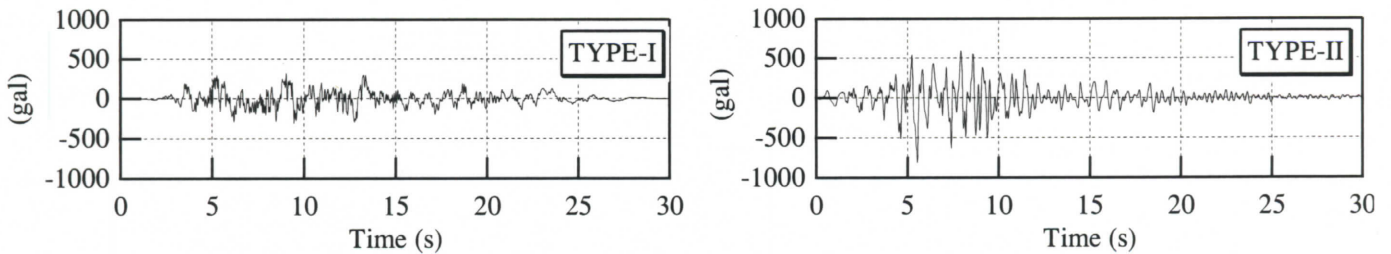


Fig.7 Input earthquake motions (2E) used in earthquake response analyses of surface soil deposits

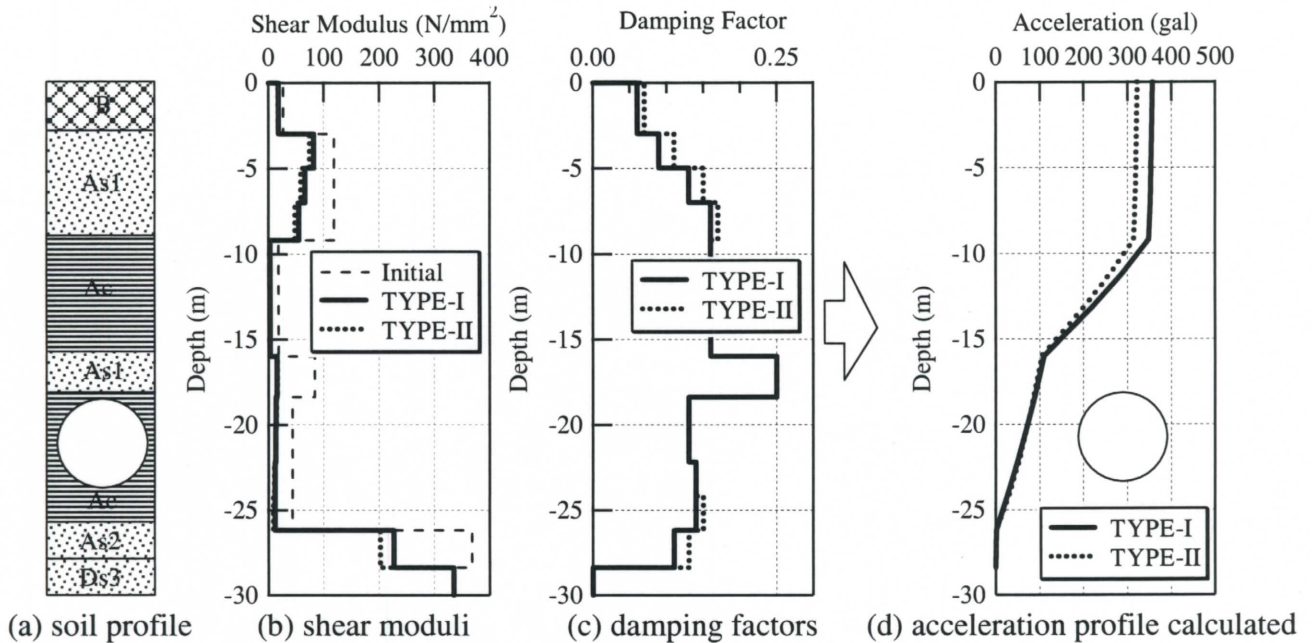


Fig.8 Dynamic properties obtained from earthquake response analyses of surface soil deposits and acceleration profiles used as an external force in axisymmetric analyses for E7T7

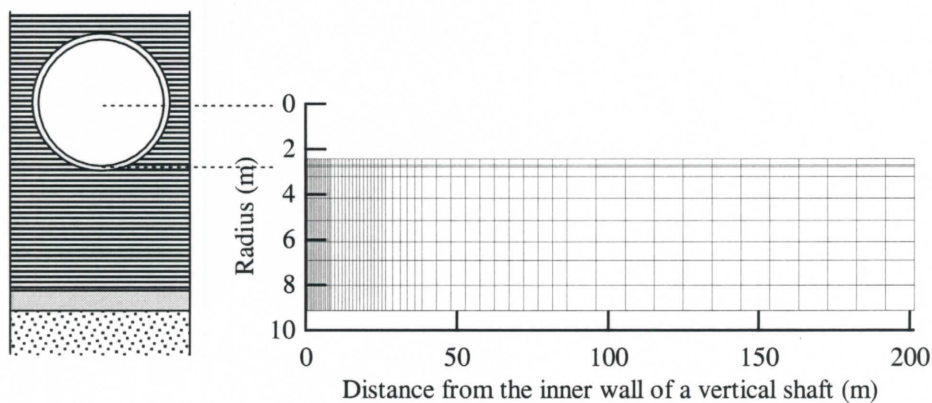


Fig.9 Axisymmetric finite element mesh for E7T7

the two types of earthquake input motions.

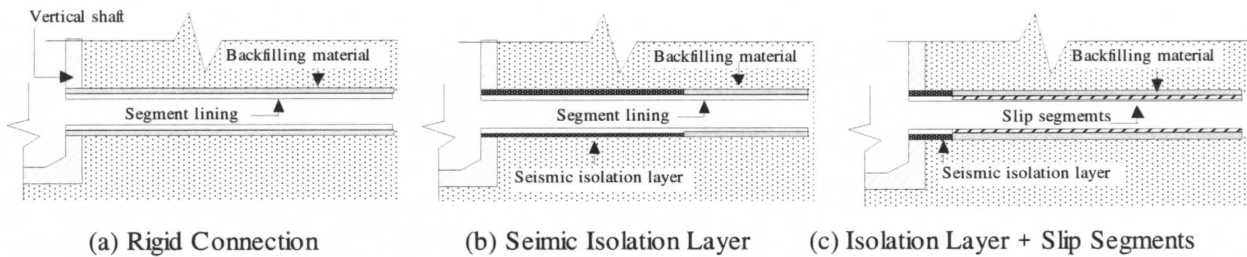
6 AXISYMMETRIC ANALYSES BY EASIT

Modeling and cases in analyses

After finishing earthquake response analyses of surface deposits at every vertical shaft, axisymmetric finite element analyses using EASIT were carried out. Fig.9 illustrates an example of a finite element mesh, modeling ground, tunnel and vertical shaft, E7T7. As shown in the figure, surface ground in a range 200 m from a vertical shaft is

modeled. The seismic load, which is a product of seismic acceleration given by Fig.8(d) and ground mass, is loaded to each nodal point with the special procedure of conversion on loading constructed for EASIT (Suzuki 2000).

Three cases of connection structures at vertical shafts as shown in Fig.10 are dealt with in the analyses. The case of seismic isolation layer denotes that a seismic isolation layer composed of SISMO-5 shown in Fig.1 is applied to the connection with a thickness of 70 mm covering segments and with a



(a) Rigid Connection (b) Seismic Isolation Layer (c) Isolation Layer + Slip Segments

Fig.10 Cases on joint structures with arrival and intermediate shafts considered in analyses

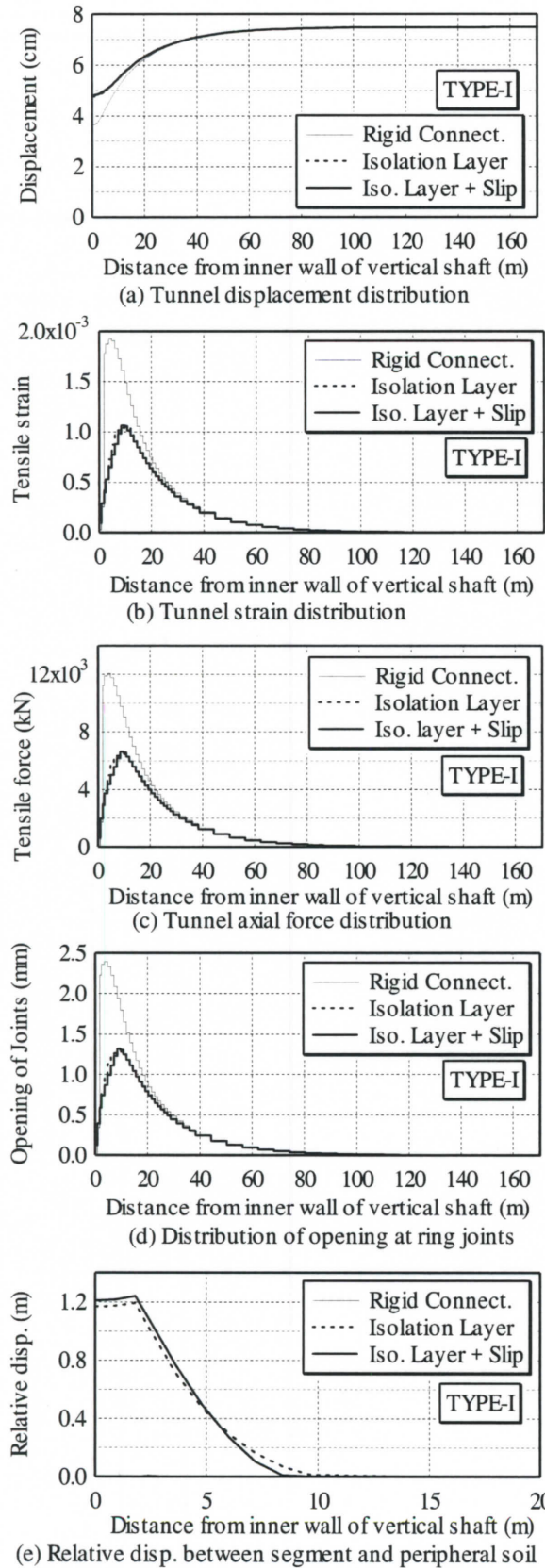


Fig.11 Results of analyses at E5T5 due to tensile deformation

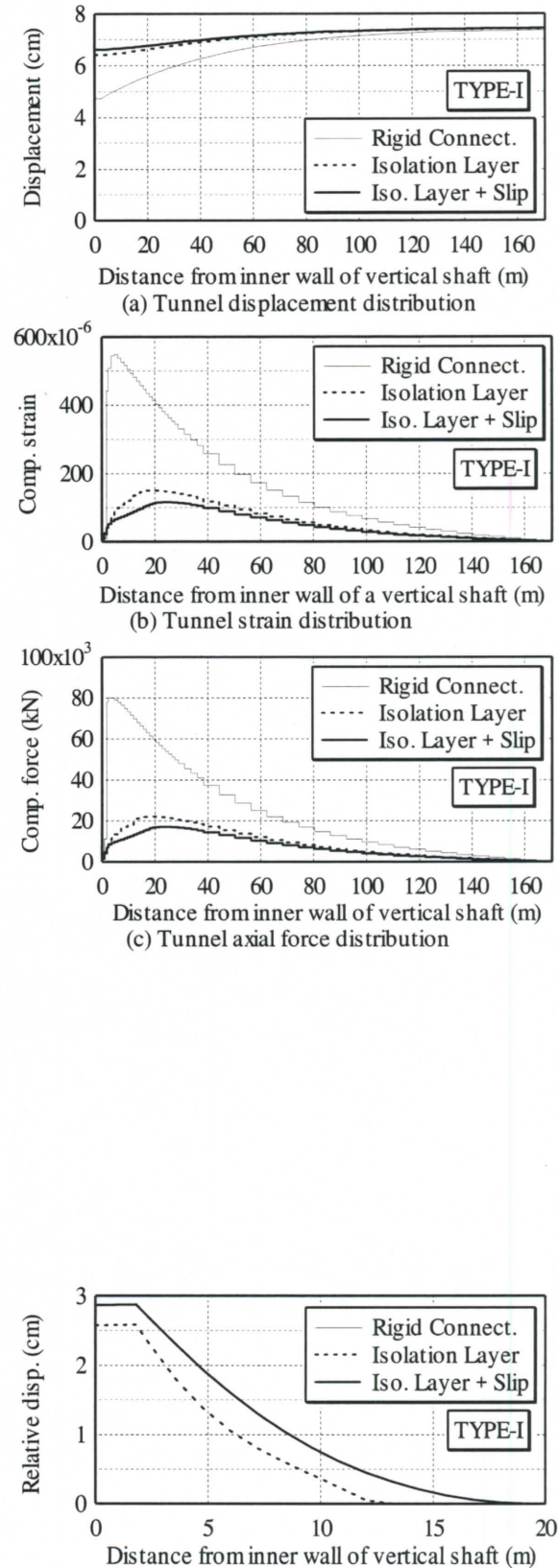


Fig.12 Results of analyses at E5T5 due to compressive deformation

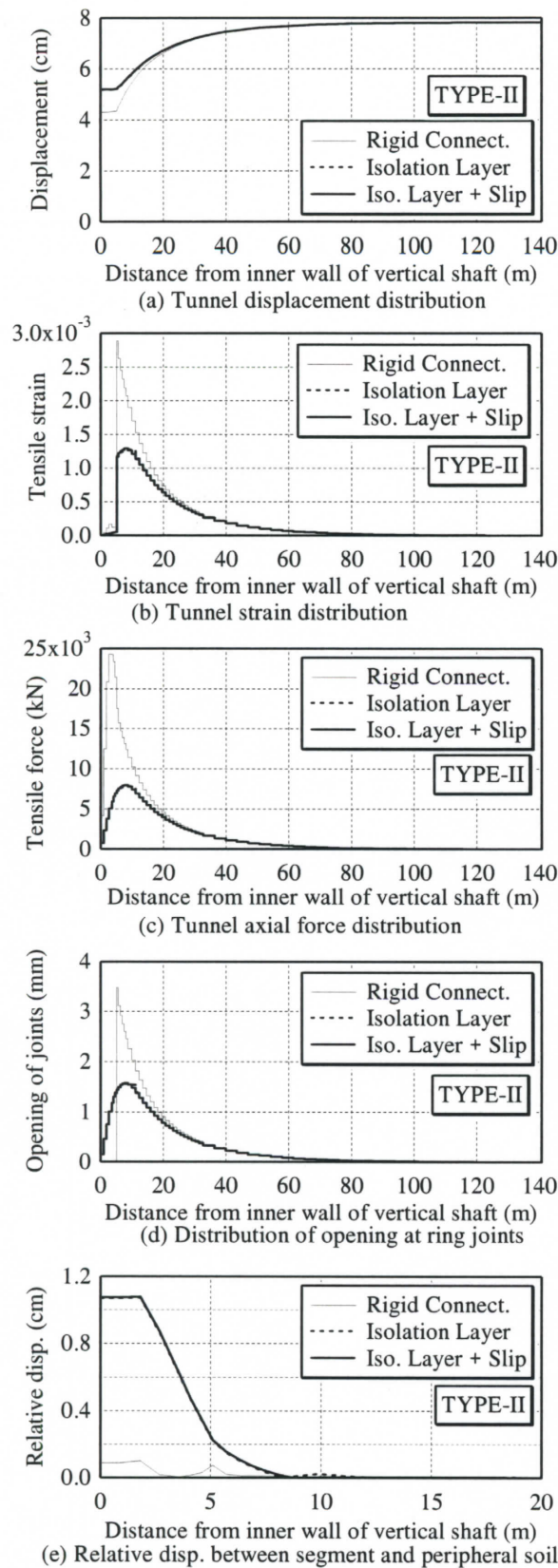


Fig.13 Results of analyses at E4T4 due to tensile deformation

total length of 10.9 m from the tunnel mouth. The case of isolation layer + slip segments, on the contrary, denotes that seismic isolation layer is applied to the connection only within the region of 2.4 m from the tunnel mouth (2 segment rings) and that slip segments are assembled from the third ring. Giving a bilinear shear stress – strain relationship to

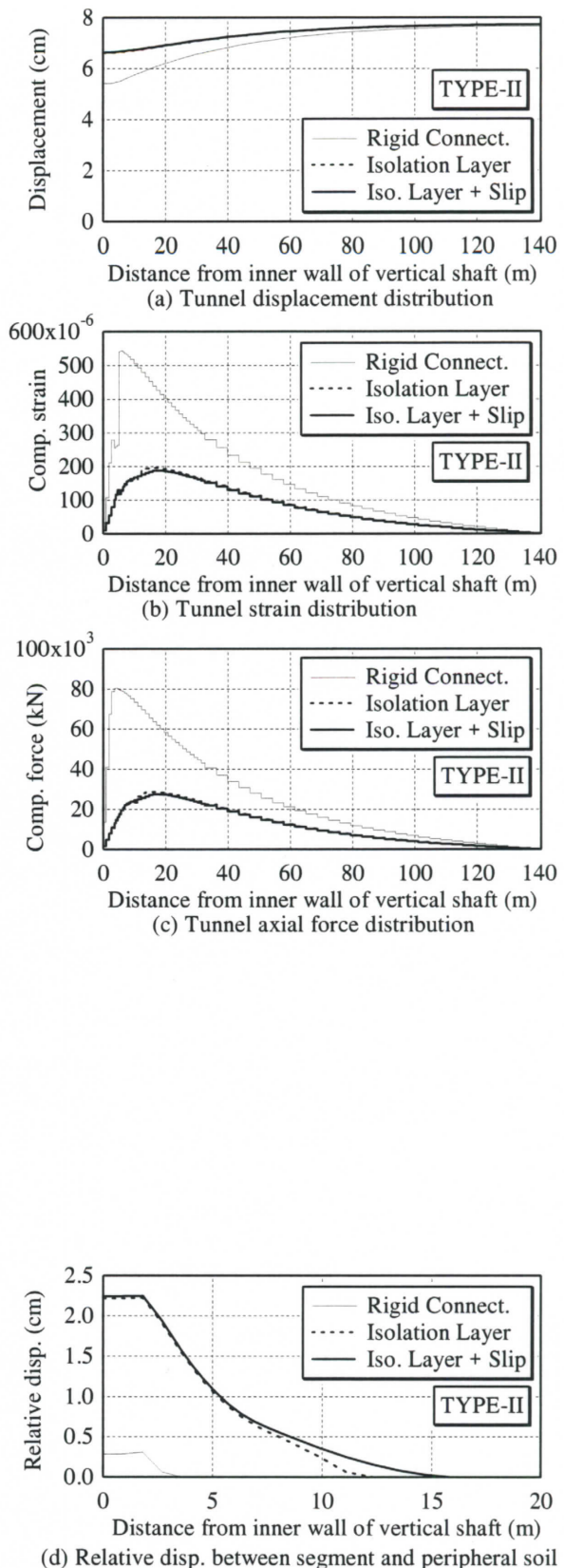


Fig.14 Results of analyses at E4T4 due to compressive deformation

thin elements covering slip segments, a slip phenomenon at the outer surface of slip segments is evaluated in EASIT as described in Chapter 3. The critical shear stress denoted by τ_f was set to be 0.35 N/mm², because values of τ_f , which is a product of a kinetic friction coefficient and an effective confining stress, were ranged from 0.32 through 0.35 N/mm²

for 7 vertical shafts. The results of analyses are described on two connections with vertical shafts, E5T5 and E4T4 which represent dynamic behaviors of intermediate shafts and an arrival shaft, respectively.

Results at E5T5

Fig.11 summarizes results of analyses by EASIT due to TYPE-I earthquake input motions in case of tensile deformation at E5T5, at which the largest response was obtained in 7 shafts. Fig.12 summarizes those in case of compressive deformation. There is a clear difference in displacement distributions between Fig.11(a) and Fig.12(a), originated from the difference in axial stiffness. It is a characteristic feature in shield-driven tunnels that the stiffness in tensile deformation is remarkably small compared to compression, because ring joints absorb displacement only in tensile deformation. Thus, the tunnel displacement sharply decreases at the connection in case of tension, while it decreases gradually in case of compression. Due to the absorption of displacement by the seismic isolation layer and slip segments, there is a clear difference in displacement distribution between the case of rigid connection and other two cases of seismic isolation in both tensile and compressive deformations.

The axial strain or axial force generated in tunnel sections is remarkably reduced by applying the seismic isolation, compared to a case of rigid connection, as shown in Fig.11(b), (c), Fig.12(b) and (c). Although the tensile stress of segments and bolts at ring joints exceeds its allowable design value in case of rigid connection, the maximum tensile force was reduced to a half compared to the case of rigid connection, in both cases of seismic isolation and combination of isolation layer + slip segments, and the tensile stresses of both segments and bolts were settled down within their design values. The maximum compressive force was reduced, on the other hand, to one fourth. The reduction rate in case of combination of isolation + slip segments is larger than that in case of seismic isolation layer, because the isolated length and absorbed displacement is larger in the former case as shown Fig.11(e) and Fig.12(d). In case of compressive deformation, however, the compressive stress of segments was settled within allowable design value, even in case of rigid connection.

The opening of ring joints exceeds its limited value of 2 mm in case of rigid connection. It can be reduced to a half in both cases of seismic isolation as

shown in Fig.11(d). The water resistance of shield-driven tunnel becomes much higher, because the seismic isolation layer is composed of water resistant material.

The above mentioned results of analyses means that the effect of combination of isolation layer and slip segments on seismic isolation is identical to or a little larger than the effect of seismic isolation layer. Due to the examination made by the authors, the seismic isolation layer was more effective than the flexible segment. Thus, the new connection structure, a combination of isolation layer and slip segments, becomes a new earthquake resistant method in place of previous methods with higher performance and lower cost.

Results at E4T4

Figs.13 and 14 summarize results of analyses due to TYPE-II earthquake input motions at the arrival shaft, E4T4 using EASIT in case of tensile and compressive deformation, respectively. There is a similar tendency in the distributions of tunnel displacement distribution and tunnel strain at E4T4 with those at E5T5. It is clear, however, that the tensile force of segments can be largely reduced by applying seismic isolation to the connection as shown in Fig.13(c). This is originated from the structural difference between intermediate and arrival shafts. The skin plate of a shield-tunneling machine composed of steel is left underground at the tunnel mouth after excavation and concrete lining is placed inside of the plate. Therefore, there is no ring joints which can absorb tensile displacement till 5.3 m toward the ground from the mouth of the tunnel, while 2 segment rings (2.4 m) are assembled inside the plate. In this section, the stiffness of tunnel lining for tension and compression is identical each other, and it is much higher than the tensile stiffness of shield segment ring.

Fig.13(d) illustrates the opening of ring joints obtained from the analyses. As mentioned above, the opening initiates at the point 5.3 m from the tunnel mouth. The maximum value of opening, 3.5 mm in case of rigid connection, can be reduced by the seismic isolation to a half, lower than its limited value.

Figs.13(e) and 14(d) show relative displacement distribution between segments of concrete lining and peripheral soil. The small amount of relative displacement of 0.2 mm can be seen at the tunnel mouth in both tensile and compressive deformation. It denotes the strain absorption by backfilling

material formed between tunnel lining and concrete wall of a vertical shaft. In tensile deformation shown in Fig.13(e), the relative displacement generates only within the skin plate in both cases of seismic isolation. Thus, no slip occurred in tensile deformation, although a slip occurs during compressive deformation as shown in Fig.14(d). Since there is not a large difference in relative displacement between the two cases of seismic isolation at E4T4 even in compressive deformation, axial force and strain of segments and lining of both cases are almost identical.

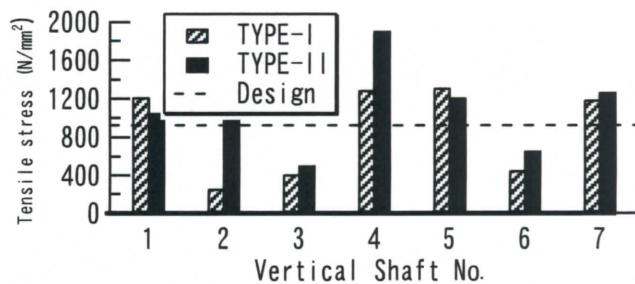
Summary of results and examinations

As a result of analyses by EASIT, it was concluded that no seismic measures are necessary for vertical shafts No.3 and 6 (E3T3 and E6T6), because every term of stress or displacement is within the design values in both tensile and compressive deformations. However, seismic isolation should be applied to the connections of residual 5 shafts, in which the bearing capacity in tensile stress of segment, tensile stress of bolts for ring joints or opening of ring joints is over the design values. Fig.16 illustrates an example of the effect of seismic isolation to the reduction of tunnel tensile stress of segments. As shown in the figure, the tensile stress of segments is reduced to the value lower than the design value by the application of seismic isolation. The effect of the seismic isolation on the reduction in tensile stress of segments is almost identical in both seismic isolation cases. Little difference in seismic isolation effects between two seismic isolation cases also can be recognized even in tensile stress of bolts and opening of ring joints.

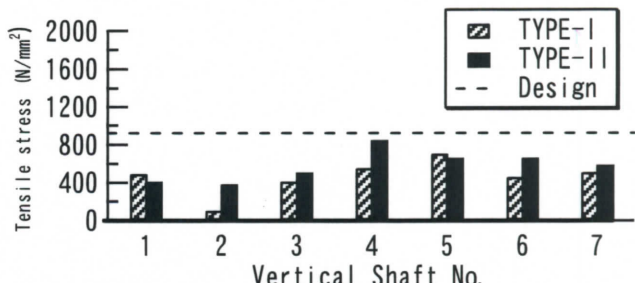
Fig.17 summarizes the total length of area where a slip generated on outer surface of slip segments, in the case of combination of isolation layer and slip segments. The largest length, 16.8 m occurs at No.5 shaft. Only small amount of length lower than 10 m occurs at other four shafts.

7 SEISMIC ISOLATION STRUCTURES

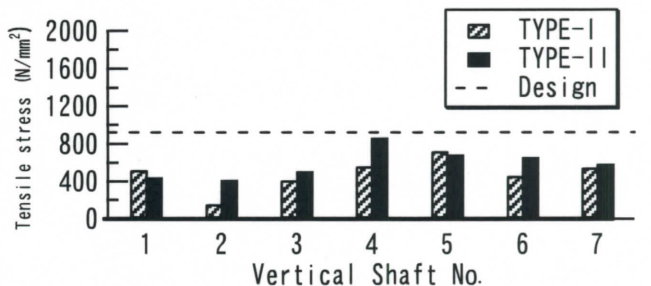
Due to the facts that the seismic isolation effect is almost identical in the two seismic isolation cases and that the total length, which is necessary to use slip segments, is relatively short, the cost performance of the combination of isolation layer and slip segments is much higher than the seismic isolation layer alone. Thus, the authors proposed that seismic isolation structures adopting the combination of isolation layer and slip segments should be applied to 5 vertical shafts.



(a) Rigid connection



(b) Seismic isolation layer



(c) Isolation layer + Slip segments

Fig.16 Reduction in axial stress of segments

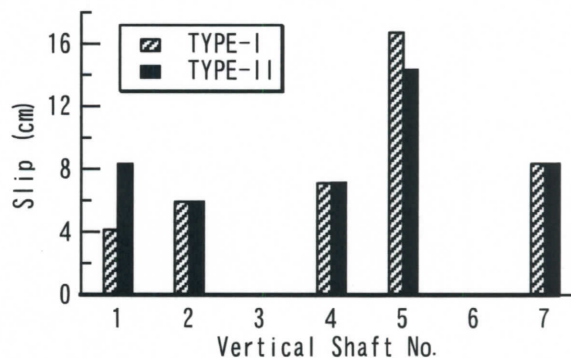


Fig.17 Slip generated on outer surface of slip segments at each vertical shaft

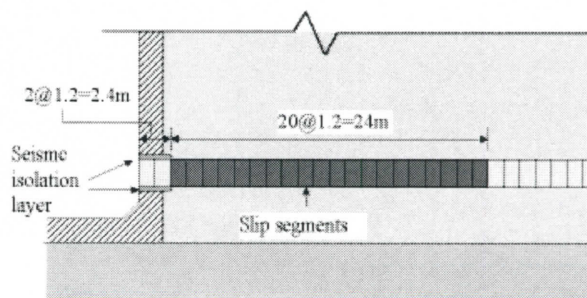
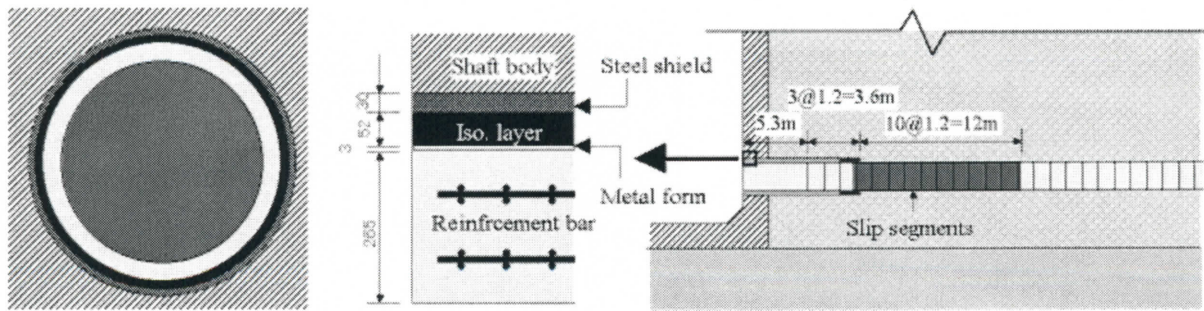


Fig.18 Schematic illustration for the seismic isolation structure at No.5 vertical shaft (E5T5)



(a) enlarged section at the tunnel mouth
 (b) seismic isolation structure proposed
 Fig.19 Schematic illustration for the seismic isolation structure at an arrival shaft, E4T4

Fig.18 illustrates a schematic representation of the seismic isolation structure designed for the connection with No.5 shaft. This represents the structure at departure and intermediate shafts. Slip segments are assembled from the mouth through the 20th segment ring which means 24 m in total length at No.5 shaft, while from the mouth through 10th segment ring (12 m) at No.1, 2 and 7 shafts.

Fig.19 illustrates a schematic representation of the seismic isolation structure proposed for the connection with No.4 arrival shaft. The seismic isolation layer is formed covering concrete lining and segments inside the skin plate, and it is also formed covering one segment ring outside the skin plate. From there, slip segments are assembled for 10 segment rings (12 m).

8 CONCLUDING REMARKS

In this paper, authors presented a seismic isolation design method and its application to connections with vertical shafts of an actual shield-driven tunnel. The conclusions derived in this paper can be summarized as follows:

- (1) The seismic isolation design in consideration of slip on outer surface of segments was applied to an actual shield-driven tunnel for the first time.
- (2) Almost same effect of seismic isolation as the application of seismic isolation layer can be obtained by the combination of isolation layer and slip segments.
- (3) The number of rings where slip segments should be assembled is at least 10 for 4 departure and intermediate shafts and 20 for one intermediate shaft, while it is 10 for an arrival shaft.
- (4) The cost performance of the combination of minimum isolation layer and slip segments is much higher than the application of seismic isolation layer or a special flexible segment, which is the standard conventional seismic measure.

REFERENCES

- Kawashima, K. et al. (1989), Research on the development of seismic design technology for underground structures, *Joint Research Reports of PWRI*, No.29, pp.208-235 (in Japanese).
- PWRI et al. (1988), Report on joint research on the development of seismic isolation materials for use in the seismic isolation design of underground structures (Part 3), *Underground Structure Seismic Isolation Design Method Manual (Draft)*, *Joint Research Reports of PWRI*, No.211 (in Japanese).
- Suzuki, T. (1989), Model vibration tests on seismic isolation structure for shield-driven tunnels, *Proc. the 20th Earthquake Engineering Symposium, JSCE*, pp.565-568 (in Japanese).
- Suzuki, T. and Tamura, C. (1995), The seismic isolation structure and the effect of seismic isolation for shield-driven tunnels, *Proc. JSCE*, No.525/I-33, pp.275-285 (in Japanese).
- Suzuki, T. (1996), Damages of urban tunnels due to the Southern Hyogo earthquake of January 17, 1995 and the evaluation of seismic isolation Effect, *Proc. the 11th World Conference on Earthquake Engineering*, Acapulco, Mexico.
- Suzuki, T. (2000), The axisymmetric finite element model developed as a measure to evaluate earthquake responses of seismically isolated tunnels, *Proc. the 12th World Conference on Earthquake Engineering*, Auckland, New Zealand, 2000.
- Suzuki, T. and Katsukawa, T. (2001a), Development of the lubricant paint applied to the seismic isolation for tunnels, *Tunnel and Underground*, Vol.32, No.6, pp.43-49 (in Japanese).
- Suzuki, T. and Katsukawa, T. (2001b), Proposal and verification tests on the seismic isolation of slip type for underground structures, *Proc. JSCE*, No.689/I-57, pp.137-151 (in Japanese).
- Tekeuchi, M. et al. (1994), Experimental study on the reduction in cross-sectional stress of shield tunnel, *Proc. JSCE*, No.483/I-26, pp.107-116 (in Japanese).
- Unjoh, et al. (1998), Seismic response control of underground structures using seismic design concept, *Proc. the 2nd Int. Conference on Structural Control*, Kyoto, Vol.2, pp.1127-1136, 1998.